

# Probing the Responsive Behavior of Polyelectrolyte Brushes Using Electrochemical Impedance Spectroscopy

Feng Zhou,<sup>†,‡</sup> Haiyuan Hu,<sup>†</sup> Bo Yu,<sup>†</sup> Vicky L. Osborne,<sup>‡</sup> Wilhelm T. S. Huck,<sup>\*,‡</sup> and Weimin Liu<sup>\*,†</sup>

State Key Laboratory of Solid Lubrication, Lanzhou Institute of Chemical Physics, Chinese Academy of Sciences, Lanzhou 730000, People's Republic of China, and Melville Laboratory for Polymer Synthesis, Department of Chemistry, University of Cambridge, Lensfield Road, Cambridge CB2 1EW, United Kingdom

Cyclic voltammetry and impedance spectroscopy were employed to probe the responsive properties of polyelectrolyte brushes. Poly[(dimethylamino)ethyl methacrylate] (PDMAEMA) brushes over 100 nm thick on gold substrates were synthesized via surface-initiated atom-transfer radical polymerization and quaternized with methane iodide to obtain cationic brushes (Q-PDMAEMA). Q-PDMAEMA brushes respond to electrolytes by exhibiting swollen and collapsed states. Swollen brushes allow good permeability of electroactive probes, while collapsed states block electron transport. Electrolytes have different impacts on the electrochemical properties of Q-PDMAEMA. Some salts (NaNO<sub>3</sub>) cause brush collapse due to charge screening, while others such as those with more hydrophobic anions (ClO<sub>4</sub><sup>-</sup>, PF<sub>6</sub><sup>-</sup>, and Tf<sub>2</sub>N<sup>-</sup>) induce brush collapse because of solubility changes. The collapsed brushes exhibit intrinsically different resistance as probed with impedance. Charged screened brushes retain good permeability to electroactive probes. Strongly coordinating hydrophobic anions lead to insoluble brushes, resulting in a high resistance. These results show that electrochemical impedance spectroscopy is a powerful technique to probe the properties and structure of polyelectrolyte brushes.

Polymer brushes are assemblies of macromolecules that are tethered by one end to a surface.<sup>1–3</sup> In dense arrays of tethered polymers the chains are forced to stretch away from the surface, opening up possibilities to create responsive surfaces if the polymer conformations can be reversibly switched between stretched and collapsed states. Recently, polyelectrolyte (PE) brushes have attracted considerable research interest, because of their response to a variety of environmental triggers such as

pH, salt concentration, and temperature.<sup>4</sup> This responsive behavior results from the incorporation and the exclusion of solvent molecules and is to a large extent governed by electrostatic interactions and osmotic pressure on the brushes.<sup>5–7</sup> This is especially true for “weak” PEs, in which the equilibrium of association–dissociation and hence distribution of charges along the polymer chain largely depends on the pH, salt concentration, and types of salts.<sup>8–10</sup> Potential applications of the swelling–collapse transition in polyelectrolyte brushes include their use as gates to control permeability in microfluidic devices,<sup>11</sup> surface coatings in chromatographic separations<sup>12–13</sup> and controlled release systems,<sup>14</sup> and artificial muscles to drive mechanical motion.<sup>15–17</sup>

A number of different experimental methods have been explored to study the conformational transitions in PE brushes including AFM,<sup>18</sup> ellipsometry,<sup>19–20</sup> and quartz crystal microbalance with dissipation (QCM-D).<sup>21–22</sup> From an electrochemical point of view, the swelling–collapse behavior will affect charge-transfer processes, the interface resistance, and the capacitance. Electro-

- (4) Rühle, J.; Ballauff, M.; Biesalski, M.; Dziezok, P.; Grohn, F.; Johannsmann, D.; Houbenov, N.; Hugenberg, N.; Konradi, R.; Minko, S.; Motornov, M.; Netz, R. R.; Schmidt, M.; Seidel, C.; Stamm, M.; Stephen, T.; Ussov, D.; Zhang, H. *Adv. Polym. Sci.* **2004**, *165*, 79.
- (5) Pincus, P. *Macromolecules* **1991**, *24*, 2912.
- (6) Zhulina, E. B.; Birshtein, T. M.; Borisov, O. V. *Macromolecules* **1996**, *28*, 1491.
- (7) Lyatskaya, Y. V.; Leermakers, F. K. M.; Fleer, G. J.; Zhulina, E. B.; Birshtein, T. M. *Macromolecules* **1995**, *28*, 3562.
- (8) Guo, X.; Ballauff, M. *Phys. Rev. E* **2001**, *64*, 051406–1.
- (9) Biesalski, M.; Johannsmann, D.; Ruehe, J. *J. Chem. Phys.* **2002**, *117*, 4988.
- (10) Zhang, H.; Rühle, J. *Macromolecules* **2005**, *38*, 4855.
- (11) Hu, S.; Ren, X.; Bachman, M.; Sims, C. E.; Li, G. P.; Allbritton, N. *Anal. Chem.* **2002**, *74*, 4117.
- (12) Kikuchi, A.; Okano, T. *Prog. Polym. Sci.* **2002**, *27*, 1165.
- (13) Liu, S.; Zhou, F.; Di, D.; Jiang, S. *Colloids Surf., A* **2004**, *244*, 87.
- (14) Kikuchi, A.; Okano, T. *Adv. Drug Delivery Rev.* **2002**, *54*, 53.
- (15) Zhou, F.; Shu, W. M.; Welland, M. E.; Huck, W. T. S. *J. Am. Chem. Soc.* **2006**, *128*, 5326.
- (16) Bumbu, G. G.; Kircher, G.; Wolkenhauer, M.; Berger, R.; Gutmann, J. S. *Macromol. Chem. Phys.* **2004**, *205*, 1713.
- (17) Abu-Lail, N. I.; Kaholek, M.; LaMattina, B.; Clark, R. L.; Zauscher, S. *Sens. Actuators, B* **2006**, *114*, 371.
- (18) Farhan, T.; Azzaroni, O.; Huck, W. T. S. *Soft Matter* **2005**, *1*, 66.
- (19) Biesalski, M.; Johannsmann, D.; Ruehe, J. *J. Chem. Phys.* **2004**, *120*, 8807.
- (20) Biesalski, M.; Ruehe, J. *Macromolecules* **2004**, *37*, 2196.
- (21) Azzaroni, O.; Sergio, M.; Farhan, T.; Brown, A. A.; Huck, W. T. S. *Macromolecules* **2005**, *38*, 10192.
- (22) Moya, S.; Azzaroni, O.; Farhan, T.; Osborne, V. L.; Huck, W. T. S. *Angew. Chem., Int. Ed.* **2005**, *44*, 4578.

\* To whom correspondence should be addressed. E-mail: wtsh2@cam.ac.uk (W.T.S.H.); wmlu@lzb.ac.cn (W.L.).

<sup>†</sup> Chinese Academy of Sciences.

<sup>‡</sup> University of Cambridge.

- (1) Edmondson, S.; Osborne, V. L.; Huck, W. T. S. *Chem. Soc. Rev.* **2004**, *33*, 14.
- (2) Advincula, R. C.; Brittain, W. J.; Caster, K. C.; Ruehe, J. *Polymer Brushes: Synthesis, Characterization, Applications*; Wiley-VCH Verlag GmbH & Co. KGaA: Weinheim, Germany, 2004.
- (3) Zhao, B.; Brittain, J. *Prog. Polym. Sci.* **2000**, *25*, 677.

chemical impedance spectroscopy (EIS) is a very effective way to probe the electron transfer and electrical properties of thin films. It has been used to quantify the defects within self-assembled monolayers (SAMs),<sup>23–30</sup> antigen–antibody interactions,<sup>31</sup> and the permeability of layered polyelectrolyte films.<sup>32–36</sup> The barrier properties of inert poly(hydroxyethyl methacrylate) (PHEMA) brushes and their derivatives were evaluated by means of EIS.<sup>37</sup> In this paper, we introduce the use of EIS as a means to study the complex behavior of polyelectrolyte brushes in response to environmental changes (different salts and concentrations). We envisage that the reversible changes in electrochemical properties of polyelectrolyte brushes will allow a further development of these brushes into a “smart” surface with switchable “gating” properties toward the permeability of electroactive molecules toward the electrode surface.

## EXPERIMENTS

**Materials.** Copper(I) bromide (99.99%) and 2, 2'-bipyridyl (BiPy, 99%) were obtained from Aldrich. NaNO<sub>3</sub>, LiClO<sub>4</sub>, NH<sub>4</sub>PF<sub>6</sub>, and (CF<sub>3</sub>SO<sub>2</sub>)<sub>2</sub>NLi (Tf<sub>2</sub>NLi) were used as electrolytes without further purification. (Dimethylamino)ethyl methacrylate (DMAEMA) was obtained from Aldrich and redistilled in the presence of CuCl before use.

**Preparation of the Polymer-Modified Electrodes.** Gold substrates were prepared by evaporating 200 nm of gold on a silicon wafer with 2 nm of chromium as the adhesive layer. Gold substrates were modified with the thiol initiator (BrC(CH<sub>3</sub>)<sub>2</sub>COO-(CH<sub>2</sub>)<sub>6</sub>SH) overnight. Polymer brushes were prepared according to a recipe of [DMAEMA]:[CuBr]:[BiPy]:[CuBr<sub>2</sub>] = 100:2:5:0.2 in MeOH/H<sub>2</sub>O (1:1) at room temperature. A typical polymerization solution is as follows: DMAEMA, 15.7 g; CuBr, 0.288 g; CuBr<sub>2</sub>, 0.0448 g; BiPy, 0.78 g; solvent, 30 mL. The solution was deoxygenated with N<sub>2</sub> for 30 min, transferred to Schlenk tube, and allowed to polymerize for overnight. After polymerization, the samples were thoroughly rinsed with Milli-Q water. Quaternization was carried out in 5 mL of iodomethane/25 mL of CH<sub>3</sub>NO<sub>2</sub> at room temperature for 24 h. The quaternized PDMAEMA [denoted as Q-PDMAEMA; PDMAEMA = poly(DMAEMA)] brush was thoroughly rinsed with solvent.

**Electrochemical Measurements.** Impedance measurements were carried out on a CHI 660B electrochemical workstation. EIS

data were simulated using the software CHI 660B. A conventional three-electrode cell was used. The reference electrode, the counter electrode, and the working electrode are saturated calomel, platinum wire, and brush-coated gold. All experiments were conducted at constant temperature. The cell was enclosed in a grounded Faraday cage with a constant area of 0.196 cm<sup>2</sup>. Impedance spectra were measured using the attached frequency response analyzer. In impedance measurement, the dc applied potential was held at an open circuit potential, and a 5 mV amplitude ac potential was applied. The voltage frequencies used for EIS measurements ranged from 10 kHz to 100 mHz. Electrochemical measurements were performed in the presence of a 1 mM K<sub>3</sub>[Fe(CN)<sub>6</sub>]/K<sub>4</sub>[Fe(CN)<sub>6</sub>] (1:1) mixture as a redox probe in 0.1 M NaNO<sub>3</sub> solution for cyclic voltammetry and in other electrolytes solutions with altering concentrations for faradic impedance measurements.

**Characterization of Polymer Brushes.** Ellipsometry measurements were performed on a DRE ELX-02C ellipsometer with a λ = 632.8 nm laser at an angle of incidence of 70° from the normal. Optical constants were measured prior to monolayer formation. A refractive index of 1.45 was used in the calculation of monolayer thickness, and a refractive index value of 1.50 was used for the brush. A minimum of four spots were measured on each sample. AFM measurements were performed using a Molecular Imaging (Phoenix, Arizona) PicoSPM, version 2.4, in MAC mode with a 1 Hz scan rate under variable applied loads. ATR-FT-IR spectra were obtained with a Perkin-Elmer Spectra One FT-IR spectrometer equipped with a universal ATR sampling accessory. Spectra were recorded with 32 scanning times and a 2 cm<sup>-1</sup> resolution.

## RESULTS AND DISCUSSION

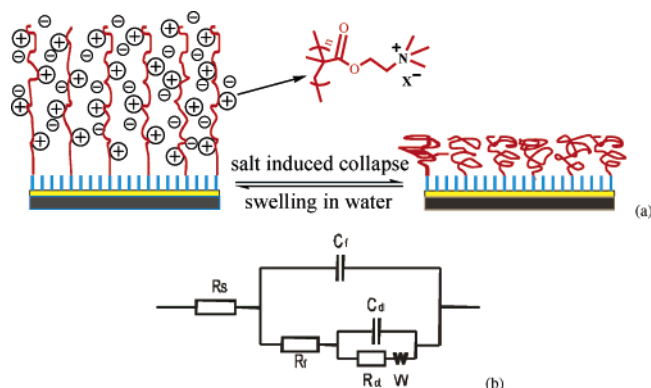
The conformational changes of polymer brushes depend on a complex interplay of factors, including polymer–polymer and polymer–solvent interactions, the degree of ionization, ion pairing, and the presence of external electrolytes. In this work, we have modified gold electrodes with surface-initiated PDMAEMA brushes using atom-transfer radical polymerization (ATRP) in aqueous conditions, which has been previously reported as a route to controlled PDMAEMA homopolymers and block copolymers.<sup>38</sup> As prepared, the PDMAEMA brushes are weak polyelectrolytes and their properties are pH dependent. The brushes were converted to strong polyelectrolytes via quaternization using iodomethane.<sup>39–41</sup> XPS analysis indicated a quaternization ratio of approximately 50% (data not shown). Typical brush thicknesses for impedance measurement are in the range of 100 nm. The reversible conformational changes are shown in Scheme 1. When polymer brushes are fully collapsed, we expect an increase in the resistance and blocking of electrochemical reactions on the electrode surface, while polymer brushes in a fully stretched state provide pathways for charge/mass transport.

Electrochemical impedance spectroscopy is an effective method to probe the resistance properties of the polymer-functionalized

- (23) Jennings, G. K.; Yong, T. H.; Munro, J. C.; Laibinis, P. E. *J. Am. Chem. Soc.* **2003**, *125*, 2950.  
 (24) Boubour, E.; Lennox, R. B. *Langmuir* **2000**, *16*, 4222.  
 (25) Sabatini, E.; Rubinstein, I. *J. Phys. Chem.* **1987**, *91*, 6663.  
 (26) Sabatini, E.; Rubinstein, I.; Maoz, R.; Sagiv, J. *J. Electroanal. Chem.* **1987**, *219*, 365.  
 (27) Finklea, H. O.; Snider, D. A.; Fedyk, J.; Sabatini, E.; Gafni, Y.; Rubinstein, I. *Langmuir* **1993**, *9*, 3660.  
 (28) Protsailo, L. V.; Fawcett, W. R.; Russell, D.; Meyer, R. L. *Langmuir* **2002**, *18*, 9342.  
 (29) Bandyopadhyay, K.; Liu, S. G.; Liu, H. Y.; Echegoyen, L. *Chem.—Eur. J.* **2000**, *6*, 4385.  
 (30) Bandyopadhyay, K.; Liu, H. Y.; Liu, S. G.; Echegoyen, L. *Chem. Commun.* **2000**, 141.  
 (31) Lasseter, T. L.; Cai, W.; Hamers, R. J. *Analyst* **2004**, *129*, 3.  
 (32) Barreira, S. V. P.; Garcia-Morales, V.; Pereira, C. M.; Manzanares, J. A.; Silva, F. J. *Phys. Chem. B* **2004**, *108*, 17973.  
 (33) Harris, J. J.; Bruening, M. L. *Langmuir* **2000**, *16*, 2006.  
 (34) Han, S.; Lindholm-Sethson, B. *Electrochim. Acta* **1999**, *45*, 845.  
 (35) Pardo-Yissar, V.; Katz, E.; Lioubashevski, O.; Willner, I. *Langmuir* **2001**, *17*, 1110.  
 (36) Lindholm-Sethson, B. *Langmuir* **1996**, *12*, 3305.  
 (37) Jennings, G. K.; Brandy, E. L. *Adv. Mater.* **2004**, *16*, 198.

- (38) Du, J.; Armes, S. P. *J. Am. Chem. Soc.* **2005**, *127*, 12800.  
 (39) Büttin, V.; Armes, S. P.; Billingham, N. C. *Macromolecules* **2001**, *34*, 1148.  
 (40) Vamvakaki, M.; Unali, G.-F.; Büttin, V.; Boucher, S.; Robinson, K. L.; Billingham, N. C.; Armes, S. P. *Macromolecules* **2001**, *34*, 6839.  
 (41) Lee, S. B.; Koepsel, R. R.; Morley, S. W.; Matyjaszewski, K.; Sun, Y.; Russell, A. J. *Biomacromolecules* **2004**, *5*, 877.

**Scheme 1. (a) Schematic Depiction of Reversible Conformational Changes of Surface-Tethered Cationic Polyelectrolyte Brushes and (b) the Equivalent Circuit Used for Fitting Electrochemical Impedance Spectra of Brush-Modified Substrates<sup>a</sup>**



<sup>a</sup>  $R_s$  = solution resistance,  $R_f$  = brush resistance,  $C_f$  = brush capacitance,  $R_{CT}$  = charge-transfer resistance,  $C_{dl}$  = double layer capacitance, and  $W$  = Warburg impedance.

electrodes. The complex impedance  $Z$  can be presented as the sum of the real,  $Z'$ , and imaginary,  $Z''$ , components that originate mainly from the resistance and capacitance of the cell, respectively.<sup>42–48</sup> Therefore, the complex impedance can be expressed as  $Z = Z' - iZ''$  and calculated by  $|Z| = [(Z')^2 + (Z'')^2]^{1/2}$ . The modification of the metallic surface, i.e., gold, with an organic layer decreases the double layer capacitance and introduces a barrier for the interfacial electron transfer. The electron-transfer resistance at the electrode usually contains the electron-transfer resistance of the unmodified electrode and the variable electron-transfer resistance introduced by the modifier in the presence of the soluble redox probe. A typical shape of an electrochemical impedance spectrum (presented in the form of a Nyquist plot,  $Z''$  vs  $Z'$  at variable frequencies) includes a semicircle region lying on the  $Z'$  axis followed by a straight line (Figure S1, Supporting Information). The semicircle portion, at higher frequencies, corresponds to the electron-transfer kinetics of the redox probe at the electrode interface, whereas the linear part at the lower frequency range is characteristic of diffusion-limited electron-transfer processes. The diameter of the semicircle corresponds to the interfacial resistance at the electrode surface, the value of which depends on the dielectric and insulating characteristics of the surface layer.

A suitable equivalent circuit must be carefully selected to reflect the real electrochemical process and to enable a fit producing accurate values.<sup>49</sup> For bare gold and initiator-modified surfaces, simplified circuits were used (for initiator-modified gold, the Randles model was used, in which charge-transfer resistance is in parallel with double layer capacitance; bare gold data were fitted

with solution resistance in series with double layer capacitance).<sup>47</sup> The circuit shown in Scheme 1 gave the best fitting results for brush-modified surfaces, contains two time constants, and includes the ohmic resistance of the electrolyte solution ( $R_s$ ), film resistance ( $R_f$ ), film capacitance ( $C_f$ ), double layer capacitance ( $C_{dl}$ ), charge-transfer resistance ( $R_{ct}$ ), and Warburg impedance ( $W$ ) resulting from the diffusion of charged species from the bulk of the electrolyte solution to the interface and through the interface layer.  $R_s$  reflects the bulk properties of the electrolyte solution and is usually not affected by composition changes occurring at the electrode surface.

**Electrochemical Verification of Brush Formation and Subsequent Derivation.** The cyclic voltammograms of  $\text{Fe}(\text{CN})_6^{3-/4-}$  (Figure 1a) show that redox reactions easily occurred on the bare gold electrode, evidenced by very large redox currents. The shape of the cyclic voltammogram demonstrates a quasi-infinite diffusion process. Modification by any organic film greatly reduced the electrode current, indicating (nearly) complete surface coverage and effective barrier formation to the redox label in the electrolyte solution. Initiator SAMs displayed a large electron-transfer barrier, and only limited current was found, probably caused by charge transport via tunneling or diffusion via defects to the electrode.<sup>50–51</sup> For a PDMAEMA brush (100 nm thick) coated gold surface, the redox response of  $\text{Fe}(\text{CN})_6^{3-/4-}$  is greatly weakened compared to that of bare gold, but enhanced compared to that of initiator-modified electrodes. We assume that the PDMAEMA brushes are in a collapsed configuration due to the poor solubility of PDMAEMA in water. Q-PDMAEMA showed a much larger electrode current indicative of brush swelling, allowing redox species to diffuse more easily within the brushes.

The impedance spectra are shown in Figure 1b and corroborate the cyclic voltammetry (CV) data; the initiator SAM has the largest radius, corresponding to a resistance of  $2.64 \times 10^5 \Omega$ . Formation of brushes on top of the SAM leads to a lower interface resistance, and quaternization of PDMAEMA further decreases the resistance from 1225 to 248  $\Omega$ . This indicates a good affinity of the quaternized brushes for solution and redox species, as well as reduced insulation properties compared with those of initiator SAMs.

**Salt-Dependent Impedance.** The electrical resistances of Q-PDMAEMA brushes in different concentrations of  $\text{NaNO}_3$  as a charge-screening salt were analyzed with CV and electrochemical impedance spectroscopy (Figure 2). CV data show that the electrical response of the redox label was hardly affected by the presence of  $\text{NaNO}_3$ . We explain this by assuming that at low salt concentrations, Q-PDMAEMA brushes remain in the swollen state, and the quasi-reversible redox wave for the redox label in solution implies no diffusion limitations and effective electrical communication between the redox label and the electrode support. Surprisingly, the polymer brushes at high salt concentrations (i.e., in a collapsed state, Figure 3a) also showed good communication between the electrode surface and the redox label. It is presumed that, even at high salt concentrations, significant amounts of water remain in the brushes and the redox species are able to penetrate through the films rather easily (perhaps the concentration at the

(42) Yan, F.; Sadik, A. O. *J. Am. Chem. Soc.* **2001**, *123*, 11335.

(43) Katz, E.; Wilmer, I. *Electroanalysis* **2003**, *15*, 913.

(44) Li, C. Z.; Long, Y. T.; Lee, J. S.; Kraatz, H.-B. *J. Phys. Chem. B* **2003**, *107*, 2291.

(45) Randles, J. E. B. *Discuss. Faraday Soc.* **1947**, *1*, 11.

(46) Finklea, H. O.; Avery, S.; Lynch, M.; Furttsch, T. *Langmuir* **1987**, *3*, 409.

(47) Janek, R. P.; Fawcett, W. R.; Ulman, A. *Langmuir* **1998**, *14*, 3011.

(48) Barsoukov, E.; Macdonald, J. R. *Impedance Spectroscopy: Theory, Experiment and Applications*; Wiley: NJ, 2005.

(49) Bai, D.; Habersberger, B. M.; Jennings, G. K. *J. Am. Chem. Soc.* **2005**, *127*, 16486.

(50) Brust, M.; Bethell, D.; Kiely, C. J.; Schiffrin, D. J. *Langmuir* **1998**, *14*, 5425.

(51) Su, L.; Gao, F.; Mao, L. *Anal. Chem.* **2006**, *78*, 2651.

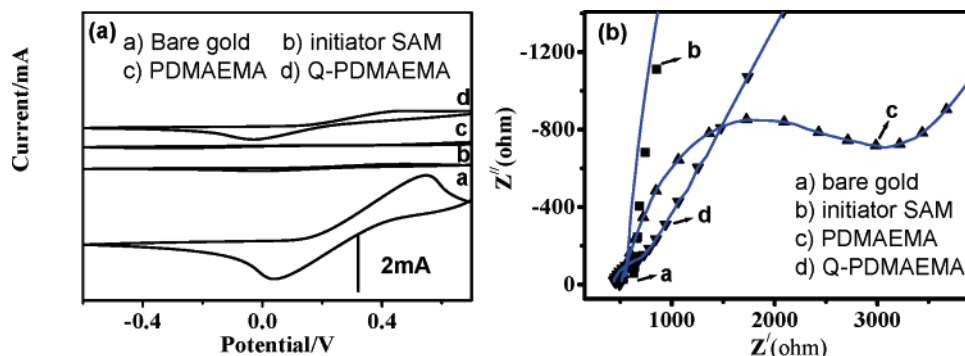


**Figure 1.** (a) Cyclic voltammograms of  $\text{Fe}(\text{CN})_6^{3-/4-}$  on different electrodes: bare gold, initiator SAM, an as-prepared PDMAEMA-functionalized electrode, and a Q-PDMAEMA brush. (b) Impedance spectra of the redox label on four surfaces. The spectra were obtained in a solution containing 1 mM  $\text{Fe}(\text{CN})_6^{3-/4-}$  (1:1) and 0.1 M  $\text{NaNO}_3$ .

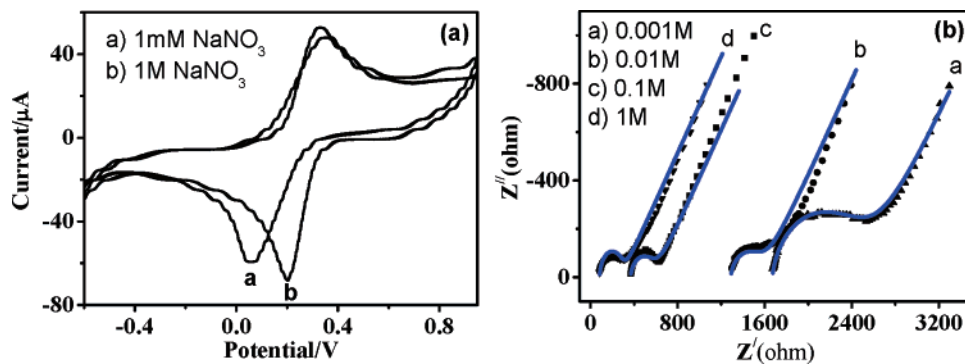


**Figure 2.** (a) Cyclic voltammogram and (b) Nyquist plots of a Q-PDMAEMA brush at different  $\text{NaNO}_3$  concentrations. Solution conditions for CV: 1 mM  $[\text{Fe}(\text{CN})_6]^{3-/4-}$  (1:1) mixture as the redox probe in a 0.1 M  $\text{NaNO}_3$  solution. The impedance was obtained at the formal potential of  $[\text{Fe}(\text{CN})_6]^{3-/4-}$  versus SCE with different salt concentrations. In all cases the measured data points are shown as symbols with the calculated fit to the equivalent circuit as a solid line.

surface is even enhanced due to the decreased brush thickness).<sup>52,53</sup>

Figure 2b shows the electrochemical impedance spectra of the salt-induced collapsed states of Q-PDMAEMA, and the fitted data are listed in Table 1. The spectra show characteristic semicircles at high frequencies and linear parts at low frequencies. Increasing the concentration of the supporting electrolyte resulted in a decrease of the semicircle radii, which is an indication of reduced interfacial resistance. This is consistent with CV results. It should be noted at this point that the impedance of bare gold decreased with an increase of the ion strength of the electrolyte solution, regardless of the nature of the salt, due to reduced thickness of the double layer at the electrode–solution interface (data not shown). Clearly, collapse of brushes does not necessarily lead to blocking of transport, since the electrolyte and redox probes can be incorporated in the collapsed brushes, which remain sufficiently hydrated to allow mobility of ions. However, brush collapse does lead to a decrease in film capacitance from 1.57 to 1.01  $\mu\text{F}$  from  $10^{-3}$  to 1 M, which may be caused by partial exclusion of (higher dielectric constant) water and a decrease in charge density. The hydrated state of charge-screened polymer brushes was verified with load-dependent AFM analysis of patterned Q-PDMAEMA brushes ( $\sim 70$  nm dry thickness) (Figure 3b). When the applied loads were increased, the height of charge-screened Q-PD-

MAEMA brushes gradually decreased, indicating penetration of the AFM tip into a soft and hydrated brush.

We then studied the effects of relatively hydrophobic anions on the interfacial electrochemistry using  $\text{LiClO}_4$ ,  $\text{NH}_4\text{PF}_6$ , and  $\text{Tf}_2\text{N}^-$  as the electrolytes, which, as we recently discovered, considerably change the nature of the brush collapse (i.e., via ion pairing rather than charge screening).<sup>21,22</sup> After anion exchange, brushes became more hydrophobic. The corresponding advancing water contact angles of Q-PDMAEMA brushes after coordination with  $\text{ClO}_4^-$ ,  $\text{PF}_6^-$ , and  $\text{Tf}_2\text{N}^-$  are  $73^\circ$ ,  $87^\circ$ , and  $93^\circ$ , respectively, while that of Q-PDMAEMA- $\text{NO}_3$  is only  $52^\circ$ . Q-PDMAEMA- $\text{Tf}_2\text{N}$  showed the highest contact angle, similar to experiments on self-assembled monolayers associated with different anions.<sup>54–55</sup> The interaction of different electrolytes with polyelectrolytes can be explained by referencing the well-known Hofmeister series.<sup>56</sup> The wettability change is due to conformational changes of the polymer chains and changes in hydration states resulting from strongly associated counterions.

The interaction of the Q-PDMAEMA brush with different electrolytes was further investigated with ATR-FT-IR (Figure 4) and AFM. After anion exchange with  $\text{ClO}_4^-$ ,  $\text{PF}_6^-$ , and  $\text{Tf}_2\text{N}^-$  the FT-IR spectra showed significant changes. Characteristic peaks attributable to respective anions appeared, for example, at 1113

(52) Braun, H.; Storck, W.; Doblhofer, K. *J. Electrochem. Soc.* **1983**, *130*, 807.  
 (53) Kulesza, P. J.; Dickinson, V. E.; Williams, M. E.; Hendrickson, S. M.; Malik, M. A.; Miecznikowski, K.; Murray, R. W. *J. Phys. Chem. B* **2001**, *105*, 5833.

(54) Lee, B. S.; Chi, Y. S.; Lee, J. K.; Choi, I. S.; Song, C. E.; Namgoong, S. K.; Lee, S-g. *J. Am. Chem. Soc.* **2004**, *126*, 480.  
 (55) Chi, Y. S.; Lee, J. K.; Lee, S-G.; Choi, I. S. *Langmuir* **2004**, *20*, 3024.

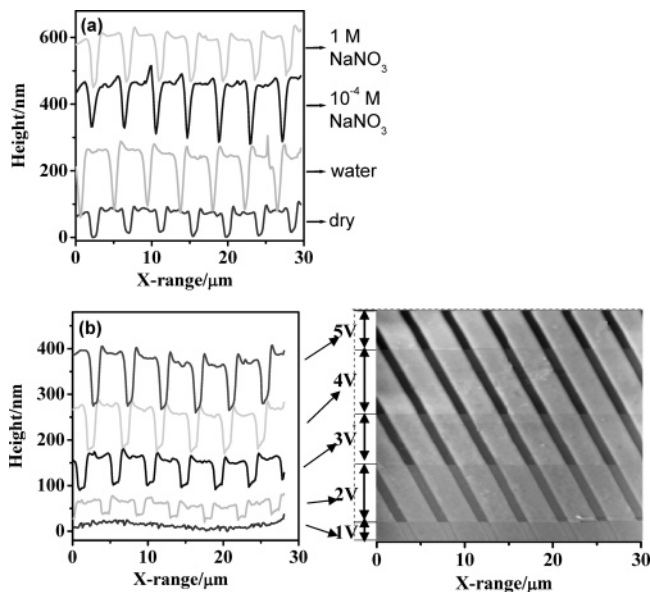


**Figure 3.** (a) AFM profile analysis of swelling/collapse of patterned Q-PDMAEMA under different conditions. Q-PDMAEMA brushes swell from  $\sim 70$  nm (dry thickness) to  $\sim 180$  nm in water, while collapsing in 1 M concentrations of electrolyte salt ( $\sim 140$  nm). A low ( $10^{-4}$  M) salt concentration has little effect on the brush thickness ( $\sim 175$  nm). (b) Effect of applied loads on the height of the Q-PDMAEMA brush in a 1 M  $\text{NaNO}_3$  solution. The set point of 5 V is the minimum applied potential to obtain a clear image, indicating slight contact between the AFM tip and the brush and no apparent penetration of the AFM tip. A decrease in the set point value means an increase of the applied force.

**Table 1. Summary of the Circuit Element Values for Q-PDMAEMA Brushes in the Presence of Different Electrolytes with Different Concentrations of  $\text{NaNO}_3$**

concn (M)	$R_s$ ( $\Omega$ )	$C_f$ ( $\mu\text{F}$ )	$R_f$ ( $\Omega$ )	$R_{ct}$ ( $\Omega$ )
1	82.21	1.067	66.23	87.04
0.1	371	1.211	187.4	107.4
0.01	1297	1.54	137.4	140.7
0.001	1674	1.57	485.4	352.3

$\text{cm}^{-1}$  for  $\text{ClO}_4^-$ ,  $865 \text{ cm}^{-1}$  for  $\text{PF}_6^-$ ,<sup>57</sup> and 1359, 1211, and  $1060 \text{ cm}^{-1}$  for  $\text{Tf}_2\text{N}^-$ .<sup>58</sup> AFM images in 0.1 M solutions of  $\text{NH}_4\text{PF}_6$  and  $\text{Tf}_2\text{NLI}$  are presented in Figure 5. The polymer brushes exhibited a decrease in thickness from 180 nm in pure water to about 145 nm in both salt solutions. Further increases in salt concentration did not lead to further changes, indicating fully collapsed brushes (although the electrochemical data above suggest that the electrolyte solution can still penetrate the brush layer in the presence of the  $\text{NaNO}_3$  solution). The fully collapsed states were further probed by increasing the load during AFM imaging, as shown in Figure 5b. Unlike the response under  $\text{NaNO}_3$  solution, increasing the applied loads during AFM measurement under 0.1

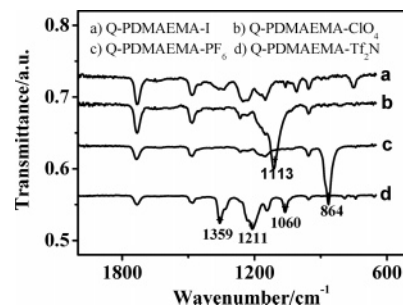


**Figure 4.** ATR-FT-IR spectra of Q-PDMAEMA-I, Q-PDMAEMA- $\text{ClO}_4$ , Q-PDMAEMA- $\text{PF}_6$ , and Q-PDMAEMA- $\text{Tf}_2\text{N}$ . Anion exchange was achieved by soaking Q-PDMAEMA-I brushes in 0.1 M solutions of the respective electrolytes for 1 h and rinsing with deionized water.

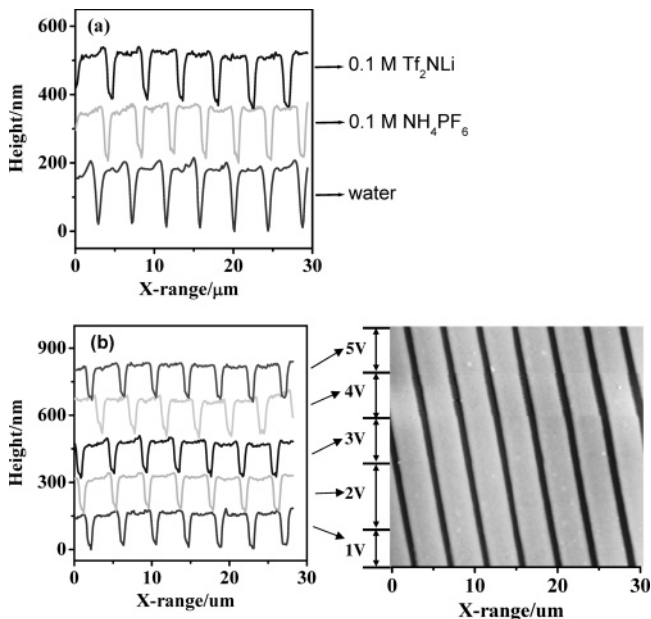


**Figure 5.** (a) Cross-section profile analysis of Q-PDMAEMA brushes under water ( $\sim 180$  nm), 0.1 M  $\text{NH}_4\text{PF}_6$ , and 0.1 M  $\text{Tf}_2\text{NLI}$  (both about 145 nm). (b) Effect of the applied loads on the height of Q-PDMAEMA- $\text{PF}_6$  brushes. The loads are indicated as the set point values.

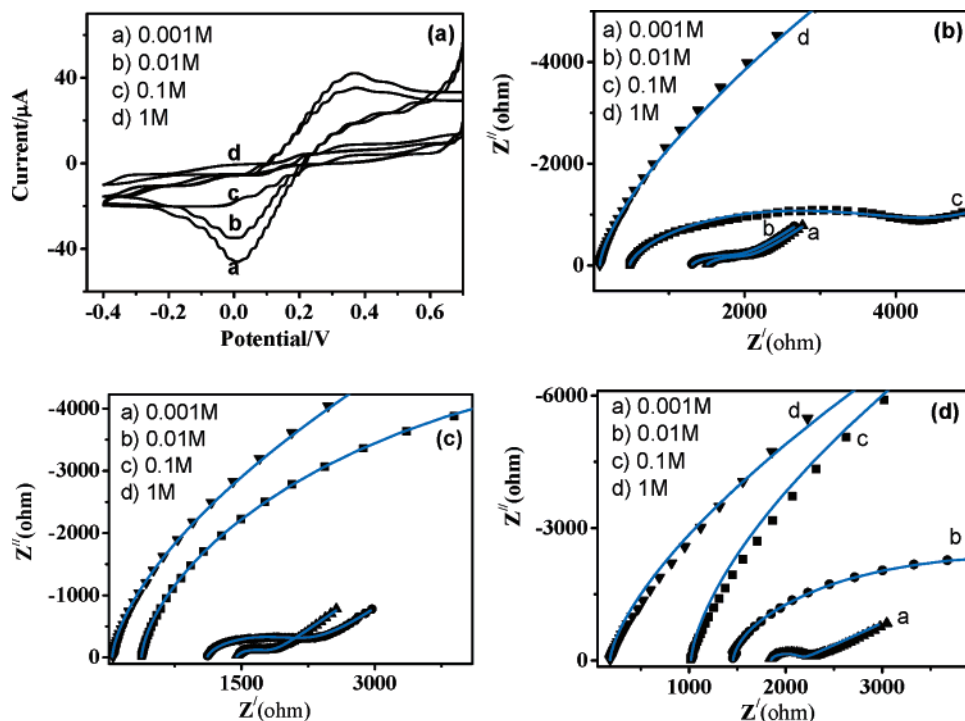
M  $\text{NH}_4\text{PF}_6$  solution left the height of the brushes essentially unchanged. We attribute this to strong ion pairing in the brush film; as a result, the films become hydrophobic and charge transport through these brushes will be largely suppressed.

Figure 6a shows the CV curves under different concentrations of  $\text{LiClO}_4$ ; the electrode current decreased dramatically with increasing salt concentrations. In 1 mM  $\text{LiClO}_4$  solution, polymer brushes showed good permeability to the redox label characterized by both large cathodic and anodic peak currents ( $-46$  and  $42 \mu\text{A}$ , respectively). Following a gradual decrease in current, a sigmoidal shaped CV was found at 1 M with no apparent redox current, indicating that the redox reaction was almost completely inhibited in 1 M  $\text{LiClO}_4$ . Two other salts, i.e.,  $\text{NH}_4\text{PF}_6$  and  $\text{Tf}_2\text{NLI}$ , showed similar results (data not shown). These experiments show that the permeability of the electroactive probe toward the electrode surface can be tuned by changing the concentrations of electrolytes, which is distinctively different from that in  $\text{NaNO}_3$  solutions. Impedance results in the form of Nyquist plots are given in Figure 6b–d. At low salt concentrations (0.001 M), Nyquist

(56) Hofmeister, F. Zur Lehre von der Wirkung der Salze. *Arch. Exp. Pathol. Pharmacol.* **1888**, *24*, 247; translated in Kunz, W.; Henle, J.; Ninham, B. W. Zur Lehre von der Wirkung der Salze. *Curr. Opin. Colloid Interface Sci.* **2004**, *9*, 19.

(57) Jung, O. S.; Kim, Y. J.; Lee, Y. A.; Park, K. M.; Lee, S. S. *Inorg. Chem.* **2003**, *42*, 844.

(58) Wen, S. J.; Richardson, T. J.; Ghantous, D. I.; Striebel, K. A.; Ross, P. N.; Cairns, E. J. *J. Electroanal. Chem.* **1996**, *408*, 113.



**Figure 6.** (a) Typical cyclic voltammograms of a Q-PDMAEMA brush under different  $\text{LiClO}_4$  concentrations in the presence of a 1 mM  $[\text{Fe}(\text{CN})_6]^{3-/4-}$  (1:1) mixture as the redox probe (scanning rate 50 mV/s). Nyquist plots ( $-Z''$  vs  $Z'$ ) of the Q-PDMAEMA brush under (b)  $\text{LiClO}_4$ , (c)  $\text{NH}_4\text{PF}_6$ , and (d)  $\text{Tf}_2\text{NLi}$  solutions of different concentrations as the supporting electrolytes. Impedance test conditions: 1 mM  $[\text{Fe}(\text{CN})_6]^{3-/4-}$  (1:1) mixture as the redox probe, 5 mV perturbation at the formal potential of  $[\text{Fe}(\text{CN})_6]^{3-/4-}$  versus SCE. In all cases the measured data points are shown as symbols with the fitted data to the equivalent circuit as solid lines.

**Table 2. Summary of the Circuit Element Values for a Q-PDMAEMA Brush in the Presence of Different Electrolytes with Different Concentrations**

electrolyte	concn (M)	$R_s$ ( $\Omega$ )	$C_f$ ( $\mu\text{F}$ )	$R_f$ ( $\Omega$ )	$R_{ct}$ ( $\Omega$ )
$\text{LiClO}_4$	1	87.7	1.211	1280	4013
	0.1	485.6	1.491	1014	1847
	0.01	1308	1.794	296.7	310.8
$\text{NH}_4\text{PF}_6$	0.001	1513	1.87	256.1	257.8
	1	57.29	1.101	4651	6480
	0.1	374.7	1.235	1241	4362
$\text{Tf}_2\text{NLi}$	0.01	1120	1.51	544.8	500.5
	0.001	1451	1.50	224	142
	1	181.1	1.014	16000	34000
	0.1	1015	1.157	6848	24000
	0.01	1453	1.486	3305	2002
	0.001	1842	1.672	170.1	215

plots displayed standard shapes, i.e., at low concentrations, semicircles at high frequencies followed by linear plots at low frequencies. With increases in  $\text{LiClO}_4$  concentration, unlike in  $\text{NaNO}_3$  solutions, the radius of the semicircles increased, indicating an increased interfacial resistance. At 1 M concentration, there seems a more linear relationship between  $Z''$  and  $Z'$ . The fitted data of all parameters are listed in Table 2. The resistance reacted more sharply to increases in concentration for  $\text{Tf}_2\text{NLi}$  solutions than for  $\text{LiClO}_4$  solutions, but generally, the resistance value follows the same order of hydrophobicity. For all electrolytes, the solution resistance decreased with increasing salt concentration. In contrast to  $\text{NaNO}_3$  solutions, both  $R_f$  and  $R_{ct}$  increased with increasing salt concentrations, and all brushes displayed a very large film resistance at high concentration, 1280, 4651, and 16000

$\Omega$  at 1 M for  $\text{LiClO}_4$ ,  $\text{NH}_4\text{PF}_6$ , and  $\text{Tf}_2\text{NLi}$ , respectively. At the same salt concentration, the values of the film resistance for these three electrolytes are again consistent with the order of hydrophobicity, indicating the different affinities for the quaternary ammonium side groups on the brushes. In all cases, the film capacitance decreased with increasing salt concentration, which is caused by gradual exclusion of water from the brushes.

It is worth noting that a collapsed brush can be recovered by soaking in  $\text{NaCl}$  and  $\text{NaNO}_3$  solutions. In fact, all impedance measurements were carried out with just one Q-PDMAEMA sample. Before the electrolyte solution was changed, the sample was treated with 1 M  $\text{NaNO}_3$  solution for 30 min and rinsed with deionized water. It was found that the brushes could be completely restored to the original values.

## CONCLUSIONS

In this paper we have demonstrated that the electrochemical study of polyelectrolyte brushes provides insight into the properties of these brushes in response to changes in the electrolyte concentration and composition. The swelling–collapse transitions, which result from switching between low and high concentrations of electrolytes, can be probed with electrochemical impedance spectra. Swelling offers fast transport of redox species to the substrate surface, while polymer brushes in collapsed states block transport. These results show how electrochemical impedance spectra can probe the internal composition of the brushes, which makes this technique complementary to ellipsometry, AFM, and FT-IR. The brushes studied here have potential uses as surfaces with tunable interface resistance. Such properties can be exploited

in smart electrochemical sensors and further extended by selective attachment of electroactive biomolecules.

#### **ACKNOWLEDGMENT**

Financial support from the NSFC (Grants 50421502 and 50405040), “973” project (Grant 2007CB607600), and EPSRC (Grant GR/T11555/01) is acknowledged.

#### **SUPPORTING INFORMATION AVAILABLE**

Impedance spectra in a Nyquist plot and Bode plots. This material is available free of charge via the Internet at <http://pubs.acs.org>.

Received for review July 21, 2006. Accepted October 24, 2006.

AC061332A